Non-Contact Vital Sign Monitoring During Sleep Through UWB Radar

Muhammad Husaini
School of Computer and Communication Engineering
Universiti Malaysia Perlis
Perlis, Malaysia
husaininadri@studentmail.unimap.edu.my

Latifah Munirah Kamarudin
School of Computer and Communication Engineering
Universiti Malaysia Perlis
Perlis, Malaysia
latifahmunirah@unimap.edu.my

Ammar Zakaria
Centre of Advanced Sensor and Technology
Universiti Malaysia Perlis
Perlis, Malaysia
ammarzakaria@unimap.edu.my

Intan Kartika Kamarudin
Department of Otorhinolaryngology Head and Neck Surgery
Universiti Teknologi MARA
Kuala Lumpur, Malaysia
kartika@uitm.edu.my

Muhammad Amin Ibrahim
Department of Internal Medicine
Faculty of Medicine
Universiti Teknologi MARA
Kuala Lumpur, Malaysia
m_amin88@uitm.edu.my

***Abstract*— To date, ultra-wideband (UWB) radar is one of the leading technologies applied in the field of non-contact vital sign monitoring. A number of studies have focused on processing reflected UWB pulse signals into breathing and heart activities; however, most have emphasised the use of stationary subjects in their data collection processes. Therefore, this paper presents a feasible study conducted to extract the human vital signs of a non-stationary subject during sleep and the optimum position of the UWB radar. The proposed algorithm could measure the respiration rate (RR) and heart rate (HR) recorded regardless of any random body movements during sleep. An analysis of the entire slow time region for the signal was performed to remove random movement signals from the subject by implementing a sinusoidal fitting algorithm to monitor the periodic movement of the chest wall. Next, the value of R-squared was used to find the fit between the algorithm and output signals, and then, the signal was transformed into a frequency domain via Fourier transform (FT). This allowed the determination of the dominant peak from the breathing and heart rates before changing to the rate per minute. An experiment was also done to monitor three different UWB radar positions (i.e. top, side, and bottom of the bed) to identify its optimum location during sleep. All results were then compared with the polysomnography signal. The result found that the top position has the lowest error rate percentage for both RR and HR with only 0.72% and 3.71%, respectively.**

Keywords*— Breathing rate, Heart rate, Non-contact, Polysomnography (PSG), Ultra-wideband (UWB) radar.

I. INTRODUCTION

Respiration rate (RR) and heart rate (HR) are crucial physiological parameters that require monitoring when tracking human vital signs. They frequently provide the first indication of any irregular physiological changes in the human body [1]. Such findings are important to avoid any deterioration of health that could reduce mortality to a great extent [2]. In particular, significant changes in vital signs could reveal possible severe medical issues in one's body. Hence, monitoring vital signs allows the detection of early symptoms and consequently increases the patient's survival rate. In many cases, the normal RR and HR of a healthy adult vary from 10 to 20 (0.16 to 0.33 Hz) breaths per minute and 40 to 120 (0.6 to 2 Hz) beats per minute, respectively [3][4]. Any rates or beats lower or higher than these values could be an early sign of physiological deterioration.

Over the past few years, the rapid advancement of wireless technology has attracted massive attention to radio frequency (RF) signals, particularly for elderly monitoring, infant vital sign monitoring, sleep monitoring, human location detection, counting, and activity recognition [5][6]. Radar sensors have become favourable as they may not require any devices attached to the body, since radar has the capabilities to wirelessly sense small physiological movements caused by respiration and heartbeat [7].

Recently, ultra-wideband (UWB)-based RF technology has allowed devices to function at frequencies between 3.1–10.6 GHz, and it has generated tremendous excitement and anticipation for wireless communication technologies. It offers much potential for civil applications, such as detecting individuals trapped under buildings in the event of natural disasters [8][9][10]. Of late, such technical benefits have attracted researchers' interest, specifically those intending to leverage its advantages for medical applications like healthcare monitoring systems, especially vital signs monitoring. The heart displaces the chest by approximately 0.08 mm in the resting state, while respiration can induce displacement varying from 1 mm to several millimetres [11]. Compared to the heart, chest displacement during breathing is more significant because of its high displacement. As such, this paper offers a feasibility analysis on implementing an impulse radio ultra-wideband (IR -UWB) radar to estimate a person's RR and HR.

Therefore, this paper presents a non-contact vital sign monitoring-based UWB radar during sleeping for detecting human RR and HR. The main contributions are:

1. This paper discusses three different radar placement locations for obtaining the optimum position of UWB radar to extract RR and HR.
2. This paper proposes combining the empty room method with a sinusoidal curve-fitting algorithm to remove random movement noise during data collection.

II. Related Works

Most vital sign measurement experiments thus far have been performed on human test subjects who are in a stationary position. However, it is unnatural for a human to remain inactive for a long-time duration. In this regard, random body movements during data collection have made it challenging for scholars to obtain vital sign signals from an individual. Thus, suggestions regarding various methods have been made to cope with noise and artefacts, including random body movement (RBM) cancellation. For example, Li and Lin [12] are the pioneer researchers who tried to solve the issue related to vital sign identification in the presence of random body motions, yielding a precise detection of the signal. The study assessed two different types of signal demodulation, complex signal demodulation and arctangent demodulation, for RBM cancellation. However, in this method, at least two antennae are required to perform detection at the front and back of the human body.

Sharafi et al. [13] implemented cross-correlation to eliminate RBMs. Each matrix row is correlated from a reflected signal with a base waveform in the time domain. Next, each waveform is shifted to the maximum correlation point. Nevertheless, this method will not work if other parts are also moving periodically. Alternatively, Koo et al. [14] developed a new algorithm for analysing range, time, and frequency to enhance the RR detection in the presence of RBMs. The algorithm works by applying a motion filter to obtain the average value before subtraction for each sample. Then, the RBM signal is eliminated via cross-correlation, detection of energy peaks, and implementation of a filtering scheme.

Also, Lazaro et al. [15] implemented the threshold method for detecting body movement before analysing the signal. The study computed a sliding window-based standard deviation with a length of 4 seconds, wherein the threshold was set at 2.5 since normal chest movement would be less than 2.5 cm. This way, any value greater than 2.5 is detected as body movement. Similarly, Khan Cho [16] implemented auto-correlation to detect various RBMs, including slightly changing head position and a tiny movement of the whole body while speaking. They measured the RBM by calculating the auto-correlation width of the signal in which movement was detected when the current width was less than half the value obtained for a stationary subject. However, this method only works for detecting RBM and does not measure the RR when the subject is moving. Also, Shang et al. [17] adopted a 2×2 IR-UWB distributed multi-input multi-output (MIMO) radar, composed of two identical radars placed in the front and back of the human torso. In addition, an adaptive moving target indication (MTI) filter was introduced to determine chest skin range displacement to cancel out the RBM. In the same year, Yang et al. [18] in their research reported that a hybrid of radar and camera system could successfully cancel the random motion noise during vital sign monitoring. Recently, Rong et al. [19] applied a method similar to [17] by placing two radars around a subject for RBM removal. However, most of the existing proposed methods only provide partial solutions for removing RBM and require an elaborate setup for the solution.

III. Method

Fig. 1 presents the flow diagram for processing the vital sign signals obtained from the UWB radar. The process started by collecting raw signals from the subject. After receiving the signal, unnecessary background noise or clutter was removed using the empty room method. Next, a sinusoidal fitting algorithm was implemented for removing any body motion before being filtered. Later, a Butterworth bandpass filter was applied to the breathing signal and heartbeat signal separation. Subsequently, the signal was transformed into the frequency domain to obtain the HR and RR values before being compared with the polysomnography (PSG) device's value to obtain the error rate.

IV. Data collection

The experimental design is illustrated in Fig. 2. It comprises a UWB radar supported by a polyvinyl chloride (PVC) bar to prevent the radar from moving or shaking. In this study, Novelda's IR-UWB radar chip X4M200 was employed to record the human respiration pattern, and an Acer Aspire laptop was used to monitor the radar chip during the data collection. The UWB radar was attached to the computer via Universal Asynchronous Receiver-Transmitter (UART), whereas MATLAB 9.11 (R2021b) software was employed to collect data and analyse BR and HR extraction signals.

During the experiment, the subject laid on the bed and slept in his preferred position while wearing the PSG device for data validation. Furthermore, during data collection, the UWB radar was placed at the top, side, and bottom of the bed, as shown in Fig. 2 (a), (b), and (c), respectively. Correspondingly, the distance between the UWB radar and

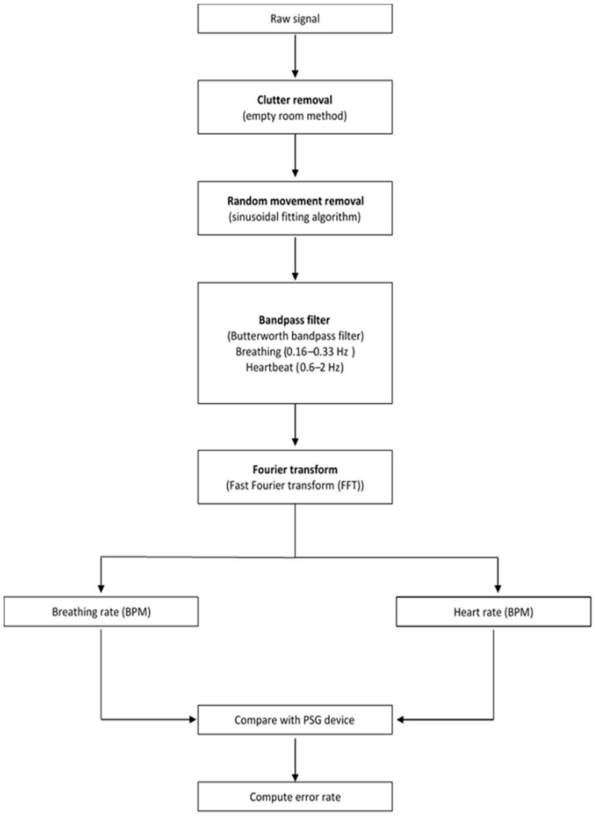

Fig. 1. Algorithm used to extract the RR and HR

subject was maintained at 0.8 m, 1 m, and 0.5 m for the top, side, and bottom positions.

Continuous pulses were sent from the radar transmitter. The receiver would receive the signals transmitted by the subject. The acquired signals were stored in a matrix form of size (m × n), where m and n denote the number of samples in slow and fast times, respectively. The obtained signal also included clutters generated from the surroundings and vital sign signals from the subject's chest. At this point, the cluttered background could be easily eliminated by applying the background subtraction method as it was assumed to be stationary, specifically by filtering the signal. This could be achieved by implementing the empty room method for detecting the location of the subject's body, which is a simple technique to remove clutter signals. The method is reflected in equation (1) as follows:

$$C_{\text{target}} = C_{receive\ signal} - C_{empty\ room} \quad (1)$$

In equation (1), $C_{receive\ signal}$ signal represents the received signal when the subject was sleeping in the bed, while $C_{empty\ room}$ shows the received signal from the UWB radar without the subject's presence in the room. C_{target} is the target signal after clutter removal. Fig. 3 shows a sample of a signal that contains the clutter and after applying the empty room method for the clutter removal for the signal. Fig. 3 (a) shows a fast time plot of a pulse transmitted from UWB radar.

Fig. 3 (a) and Fig. 3 (b) show the plot of the data matrix in the form of slow time fast time with a size m × n. The waveform with red represents a raw signal, and the waveform with blue signifies the signal after the clutter was removed. Fig. 3 (a) is before clutter removal, and Fig. 3 (b) shows the result after clutter removal was applied. From Fig. 3, it can be clearly seen that most static clutter was removed from the signal using the empty room method.

A. Random body movement removal

During data collection, it is impossible to assume that the subject will remain stationary for quite some time. Thus, a random body motion detection algorithm for removing the RBM is necessary. The breathing rhythm and chest movement can be easily recognised in a stationary state as the target body position stays at a cell range, similar to the UWB radar during data collection. However, any micro or macro random body movements (e.g. shivering or position change) during sleep may significantly affect the breathing signal. If and when this happens, the human target position will fall into several cells range. As a breathing signal may be hard to recognise during the intervening time, it is crucial to remove any artefacts caused by body motion before the signal is extracted. This problem can be solved by utilising a sinusoidal fitting algorithm to distinguish between the chest wall movement and RBM. The chest wall movement is caused by breathing, and the heart movement works in a periodic motion. Thus, the sinusoidal curve-fitting will show how much of the output

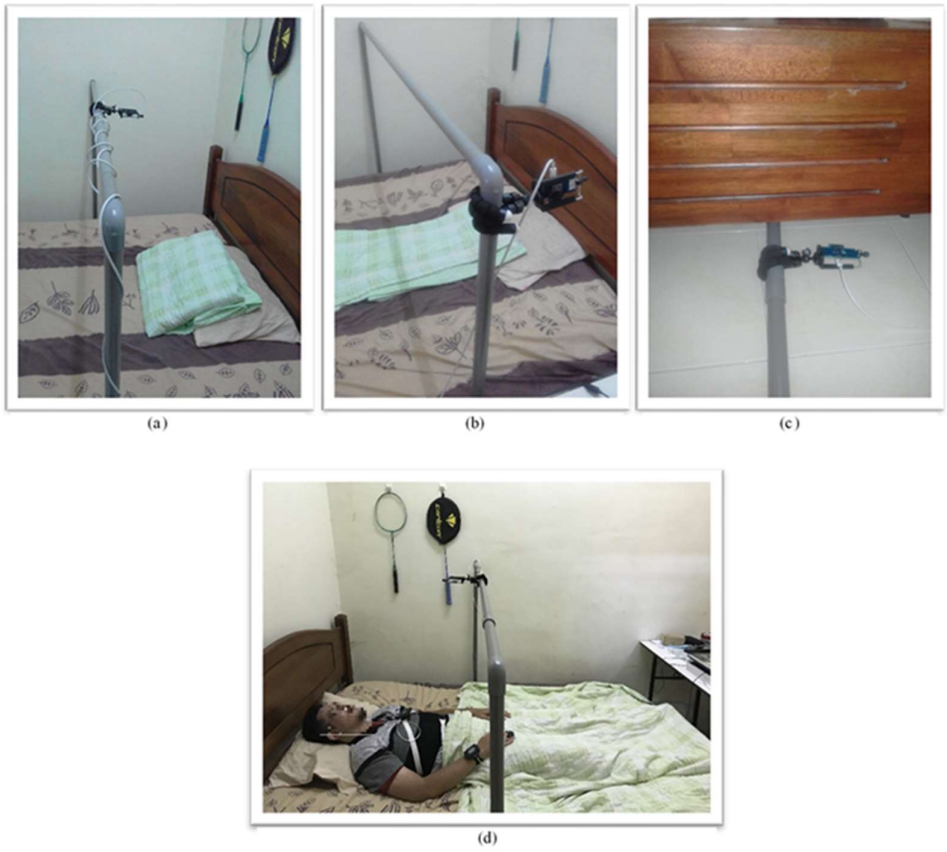

Fig. 2. Position of UWB radar: (a) Top position. (b) Side position. (c) Bottom / down position. (d) Position of UWB radar

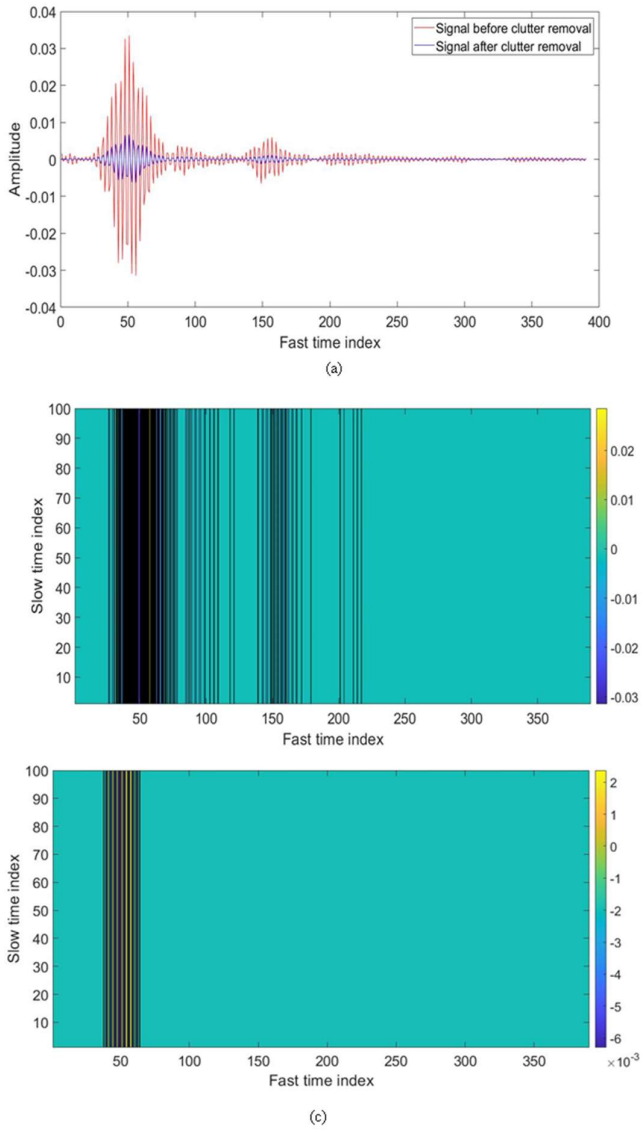

Fig. 3. (a) Received fast time signal before and after clutter removal. (b) Signal before clutter removal. (c) Signal after clutter removal.

signals fall into the sinusoidal pattern. The general form for the sum of the sinusoidal curve can be represented by:

$$y = \sum_{i=1}^{n} \alpha_i \sin(b_i x + c_i) \qquad (2)$$

where α is the amplitude, b is the frequency, c is the phase constant for each sine wave term, and n is the number of terms in the series.

The R-squared value was used for finding the fit of the signal, which is defined as follows:

$$R^2 = 1 - \frac{\sum_{i=1}^{n}(y_i - \hat{y}_i)^2}{\sum_{i=1}^{n}(y_i - \bar{y}_i)^2} \qquad (3)$$

In equation (3), y_i is the actual value of the radar signal, $\hat{y}_i$ represents the estimated values from the sinusoidal fitting algorithm, whereas $\bar{y}_i$ shows the mean of y. Here, the value of R-squared lies within the range of values between 0 and 1. A higher value would indicate that the reflected signal from UWB radar has a higher sinusoidal pattern, which could store the HR and RR. On the contrary, a lower R-squared value could suggest that the signal possesses a low sinusoidal pattern that carries an unwanted body motion signal. In this study, the threshold value for R-squared was set to 0.5. Fig. 4 shows a sample of best-fit signal from sinusoidal fitting, where Fig. 4(a) shows the R-squared value greater than 0.5 and Fig 4(b) shows the R-squared value less than 0.5. Further details are included in Fig. 4 and Algorithm 1.

Algorithm 1.

1. Apply the sinusoidal curve fit in equation (2), which would give the amplitude, frequency, and phase constant for the best fit to the raw signals.
2. Determine the R-squared value for each of the signals using equation (3).
3. Find the signals with an R-squared value exceeding 0.5.
4. Determine whether selected signals have the frequency lying in the heart and breathing frequencies or not; if yes, then save the signal.

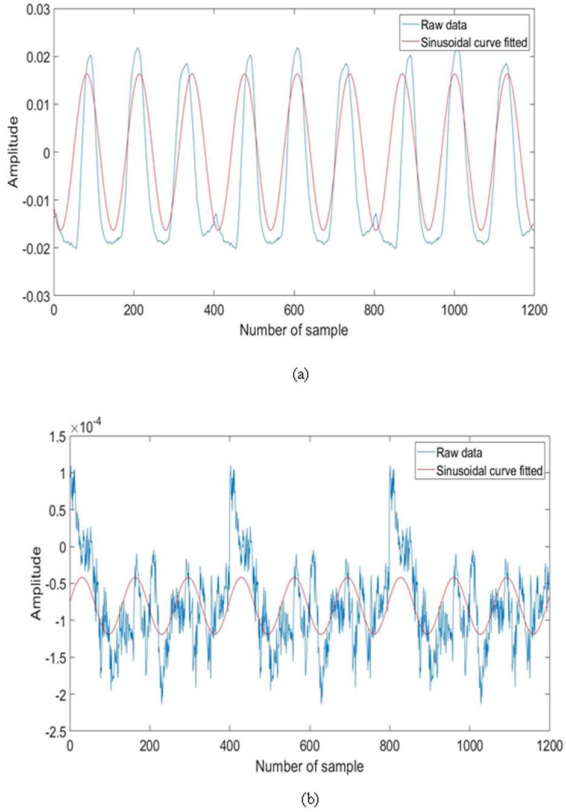

Fig. 4. Sample of best-fit signal from sinusoidal fitting. (a) R-squared value greater than 0.5. (b) R-squared value less than 0.5.

B. Fourier Transform

After removing clutter and random body motions from the signal, it was filtered using a Butterworth bandpass filter with a cut-off frequency range from 0.16–0.33 Hz and 0.6–2 Hz for the RR and HR, respectively [4]. Next, the signal was converted from a time domain to a frequency domain by applying the Fourier transform algorithm. The highest peak represents the fundamental frequency for the RR and HR. Finally, equation (4) was applied to determine the RR and HR per minute.

$$BPM = Frequency_{(Peak\ value)} \times 60 \quad (4)$$

V. Result and Discussion

To verify the result of the proposed method, a PSG device was used to monitor both RR and HR during data collection. Only a wrist oximeter and breathing belt were attached to the PSG device to measure RR and HR signals. No additional device was connected to the PSG as the purview of this study is limited to measuring HR and chest wall movement.

The experiment successfully extracted the RR and HR for 60 minutes in each trial. The error rate was used to appraise the performance of the proposed method with the actual value from the PSG device. The error rate of BPM was used to measure the accuracy of the BR and HR frequencies of the UWB radar from the PSG sensor, obtained by multiplying the values by 60. The error rate is expressed as:

$$Error\ rate = \frac{BPM_{UWB} - BPM_{PSG}}{BPM_{PSG}} \times 100 \quad (5)$$

Where BPM_{UWB} represents the beat per minute of the proposed method using UWB radar, while BPM_{PSG} represents the reference of a beat per minute for the PSG sensor.

TABLE I and TABLE II show the result of the error rate percentage between the UWB radar and PSG device for both HR and BR. The data were analysed for 60 minutes of subject's sleep time from three different radar placement positions: top, side, and down. Data collection was repeated thrice for each position and equivalent to nine days of processing.

Looking at the result in TABLE I, the UWB radar attached at the top position on the subject depicts the lowest average error rate compared to the other two positions with an RR of 0.72% from PSG. This was followed by the down and side positions at 2.10% and 2.90%, respectively. A similar pattern was observed according to the average error of HR in TABLE II. The top position yielded the lowest average error at 3.71%, followed by the down position at 6.24%. Meanwhile, the side position generated the maximum average error at 13.17%. It should be noted that the top position revealed the lowest average error rate as expected for HR and RR alike. Compared to the result of a previous study [20], the minimum average error rate obtained in this study is still within the acceptable range.

TABLE I. Error rate of breathing rate between UWB and PSG.

Position	Trial	Error rate (%)	Average (%)
Top	1	0.39	0.72
	2	1.16	
	3	0.62	
Side	1	2.71	2.90
	2	4.45	
	3	1.55	
Down	1	1.83	2.10
	2	1.95	
	3	2.53	

TABLE II. Error rate of heart rate between UWB and PSG

Position	Trial	Error rate (%)	Average (%)
Top	1	3.52	3.71
	2	4.29	
	3	3.61	
Side	1	10.64	13.17
	2	12.56	
	3	16.32	
Down	1	3.88	6.24
	2	6.81	
	3	8.04	

The result obtained in this study for both minimum average error rate for RR and HR lie within an acceptable range. In Ref. [21], a minimum error rate of 4.6% in moving state and 2.25% in resting-state was demonstrated. The result was compared with a standard ECG device. Also Culjak et al. [22] performed an experiment by integrating inertial measurement unit sensors with UWB radar for breathing monitoring. The experimental results showed that their proposed method was able to detect breathing patterns with a 10% error rate. They used Brain Products actiCHamp as a reference system for breathing estimation. Zhang et al. [23] implemented harmonic multiple loop detection (HMLD) algorithm for RR and HR detection. The algorithm's RR and HR average errors were 4.95% and 5.06%, respectively. Wang et al. [24] proposed improved convolutional sparse coding method using UWB Radar on detecting heart rate. The error rate result ranged from 1.9% to 6.6%. Duan and Liang [25] applied variational mode decomposition (VMD) algorithm-based UWB radar for extracting heartbeat signals and respiratory signals. The error rate result for breathing and heart rate signals ranged from 0% to 5% and 9% to 13%, respectively. TABLE III summarises the result performance of vital sign detection with the previous studies.

TABLE III. Results and performance comparison with the referenced algorithm

Reference	Method	Reference device	Error rate result
[21]	Variational nonlinear chirp mode decomposition	ECG	HR (2.25% - 4.6%)
[22]	Transversal UWB propagation method	Brain Products actiCHamp	BR (10%)
[23]	HMLD	Pulse oximeter (HR) Manual chest count (RR)	BR (4.95%) HR (5.06%)
[24]	Improved convolutional	Finger pulse counter (FPC)	HR (1.9% - 6.6%)

	sparse coding method		
[25]	VMD	ECG	BR (0 to 5 %) HR (9% to 13%)
This study	Empty room method Sinusoidal curve fitting	PSG	BR (0.72%) HR (3.71%)

VI. Conclusion

This study successfully implemented a reliable technique for monitoring vital signs during sleep in which the UWB radar location and non-stationary vital sign monitoring are the two main focuses. The top position yielded the lowest error rate compared to other positions tested for the breathing and heart rate data, whereas the side position was the least effective for measuring the parameters. In brief, the location played an important role in detecting proper RR and RR data.

The second objective of this study was to monitor the vital signs of a non-stationary subject. The experimental result subsequently showed that the algorithm worked perfectly in distinguishing between the RBM and chest movement.

Acknowledgement

This research is fully supported by Fundamental Research Grant Scheme (FRGS) by Ministry of Higher Education Malaysia (FRGS/1/2018/SKK06/UNIMAP/02/1).

References

[1] D. Evans, B. Hodgkinson, and J. Berry, "Vital signs in hospital patients: A systematic review," *Int. J. Nurs. Stud.*, vol. 38, no. 6, pp. 643–650, 2001, doi: 10.1016/S0020-7489(00)00119-X.

[2] C. Hands *et al.*, "Patterns in the recording of vital signs and early warning scores: Compliance with a clinical escalation protocol," *BMJ Qual. Saf.*, vol. 22, no. 9, pp. 719–726, 2013, doi: 10.1136/bmjqs-2013-001954.

[3] M. A. Russo, D. M. Santarelli, and D. O'Rourke, "The physiological effects of slow breathing in the healthy human," *Breathe*, vol. 13, no. 4, pp. 298–309, 2017, doi: 10.1183/20734735.009817.

[4] H. Chang, J. Chen, and Y. Liu, "Micro-piezoelectric pulse diagnoser and frequency domain analysis of human pulse signals," *J. Tradit. Chinese Med. Sci.*, vol. 5, no. 1, pp. 35–42, 2018.

[5] S. Shukri, L. M. Kamarudin, M. H. F. Rahiman, A. Zakaria, and D. L. Ndzi, "Device-free localization and human mapping for ambient assisted living: Radio map approach," in *2019 IEEE International Conference on Sensors and Nanotechnology*, 2019, pp. 1–4.

[6] S. Shukri and L. M. Kamarudin, "Device free localization technology for human detection and counting with RF sensor networks: A review," *J. Netw. Comput. Appl.*, vol. 97, no. September, pp. 157–174, 2017, doi: 10.1016/j.jnca.2017.08.014.

[7] C. Li *et al.*, "A method for remotely sensing vital signs of human subjects outdoors," *Sensors (Switzerland)*, vol. 15, no. 7, pp. 14830–14844, 2015, doi: 10.3390/s150714830.

[8] A. Nezirovi, A. G. Yarovoy, S. Member, and L. P. Ligthart, "Signal processing for improved detection of trapped victims using UWB radar," vol. 48, no. 4, pp. 2005–2014, 2010.

[9] J. Li, L. Liu, Z. Zeng, and F. Liu, "Advanced signal processing for vital sign extraction with applications in UWB radar detection of trapped victims in complex environments," *IEEE J. Sel. Top. Appl. Earth Obs. Remote Sens.*, vol. 7, no. 3, pp. 783–791, 2014, doi: 10.1109/JSTARS.2013.2259801.

[10] S. Karthikeyan and N. S. Renga Preethi, "Life detection system using UWB Radar during Disaster," *Proc. 2nd Int. Conf. Green Comput. Internet Things, ICGCIoT 2018*, pp. 361–365, 2018, doi: 10.1109/ICGCIoT.2018.8752992.

[11] M. Y. W. Chia, S. W. Leong, C. K. Sim, and K. M. Chan, "Through-wall UWB radar operating within FCC's mask for sensing heart beat and breathing rate," *EURAD 2005 Conf. Proc. - 2nd Eur. Radar Conf.*, vol. 2005, no. 117674, pp. 267–270, 2005, doi: 10.1109/EURAD.2005.1605615.

[12] C. Li and J. Lin, "Random body movement cancellation in doppler radar vital sign detection," *IEEE Trans. Microw. Theory Tech.*, vol. 56, no. 12, pp. 3143–3152, 2008, doi: 10.1109/TMTT.2008.2007139.

[13] A. Sharafi, M. Baboli, M. Eshghi, and A. Ahmadian, "Respiration-rate estimation of a moving target using impulse-based ultra wideband radars," *Australas. Phys. Eng. Sci. Med.*, vol. 35, no. 1, pp. 31–39, 2012, doi: 10.1007/s13246-011-0112-2.

[14] Y. S. Koo, L. Ren, Y. Wang, and A. E. Fathy, "UWB MicroDoppler Radar for human gait analysis, tracking more than one person, and vital sign detection of moving persons," *IEEE MTT-S Int. Microw. Symp. Dig.*, no. June, 2013, doi: 10.1109/MWSYM.2013.6697702.

[15] A. Lazaro, D. Girbau, and R. Villarino, "Techniques for clutter suppression in the presence of body movements during the detection of respiratory activity through UWB radars," *Sensors*, vol. 14, no. 2, pp. 2595–2618, 2014.

[16] F. Khan and S. H. Cho, "A detailed algorithm for vital sign monitoring of a stationary/non-stationary human through IR-UWB radar," *Sensors (Switzerland)*, vol. 17, no. 2, 2017, doi: 10.3390/s17020290.

[17] X. Shang, J. Liu, and J. Li, "Multiple object localization and vital sign monitoring using IR-UWB MIMO radar," *IEEE Trans. Aerosp. Electron. Syst.*, vol. 56, no. 6, pp. 4437–4450, 2020.

[18] C. Yang, B. Bruce, X. Liu, B. Gholami, and N. Tavassolian, "A hybrid radar-camera respiratory monitoring system based on an impulse-radio ultrawideband radar," in *2020 42nd Annual International Conference of the IEEE Engineering in Medicine \& Biology Society (EMBC)*, 2020, pp. 2646–2649.

[19] Y. Rong, K. V. Mishra, and D. W. Bliss, "Multiple moving targets heartbeat estimation and recovery using multi-frequency radars," in *2021 IEEE Radar Conference (RadarConf21)*, 2021, pp. 1–5.

[20] H.-S. Cho and Y.-J. Park, "Detection of heart rate through a wall using UWB impulse radar," *J. Healthc. Eng.*, vol. 2018, 2018.

[21] W. Yin, X. Yang, L. Li, L. Zhang, N. Kitsuwan, and E. Oki, "Hear: Approach for heartbeat monitoring with body movement compensation by ir-uwb radar," *Sensors*, vol. 18, no. 9, p. 3077, 2018.

[22] I. Culjak, H. Mihaldinec, Z. L. Vasic, K. Friganovic, H. Dzapo, and M. Cifrek, "A contactless human respiration rate measurement using UWB transversal propagation method," *2019 Int. Symp. Antennas Propagation, ISAP 2019 - Proc.*, 2019.

[23] Y. Zhang, X. Li, R. Qi, Z. Qi, and H. Zhu, "Harmonic multiple loop detection (HMLD) algorithm for not-contact vital sign monitoring based on ultra-wideband (UWB) radar," *IEEE Access*, vol. 8, pp. 38786–38793, 2020.

[24] P. Wang *et al.*, "Noncontact heart rate measurement based on an improved convolutional sparse coding method using IR-UWB radar," *IEEE Access*, vol. 7, pp. 158492–158502, 2019, doi: 10.1109/ACCESS.2019.2950423.

[25] Z. Duan and J. Liang, "Non-contact detection of vital signs using a UWB radar sensor," *IEEE Access*, vol. 7, pp. 36888–36895, 2019, doi: 10.1109/ACCESS.2018.2886825.